SiO Maser Movies: The Re-Run

© **M. D. Gray**[1], **M. Wittkowski**[2], **E. M. L. Humphreys**[2], **S. Yu. Parfenov**[3], **A. M. Sobolev**[3]

[1]School of Physics and Astronomy, University of Manchester, UK
[2]ESO, Garching, Germany
[3]Ural Federal University, Ekaterinburg, Russia

We report preliminary results of a new time-dependent model of SiO maser emission in the extended atmosphere of an AGB star. We compare this model to time-series observations of SiO masers towards the Mira variable TX Cam. The model masers are predominantly radiatively pumped, at least in the second half of the stellar pulsation period. Predictions for the radius of peak maser brightness and the width of the maser ring are broadly in line with the observations.

Keywords: VLBI, masers, radiative transfer, stars: AGB & post-AGB.

1 Introduction

The role of infra-red radiation and radial shock-waves in pumping circumstellar SiO masers has long been a matter of debate. One AGB star, TX Cam, has been studied in great detail with the VLBA. The 43.122 GHz $v = 1$, $J = 1 - 0$ maser line of ^{28}SiO in this star has been observed at approximately monthly intervals over a total of more than three consecutive pulsation periods [1], each of $P = 557$ d.

The complete dataset described above, comprising 78 epochs between 1997 May 24 and 2002 Jan 25, has been assembled into a short movie of 112 frames that demonstrates the evolution of the SiO maser zone of TX Cam. The basic pattern of an irregular ring of maser objects surrounding the star is maintained throughout, and this ring appears to expand and contract, though contraction is absent in the first observed period. There are also other substantial cycle-specific variations in kinematics and structure [1]. The TX Cam movie itself is deposited as*.

Attempts to provide a theoretical/computational counterpart to the movie described above began with a one period model [2], based on hydrodynamic solutions from [3]. This model successfully reproduced the observed broken ring structure, but unfortunately had an unknown relation between the optical light curve and shock-waves produced by the stellar pulsation. An improved model [4] incorporated hydrodynamic solutions from [5], which fixed the shock cycle to the optical light

*http://mnras.oxfordjournals.org/lookup/suppl/doi:10.1093/mnras/stt954/-/DC1

curve, but still relied on the large velocity gradient (LVG) approximation for the maser solutions, and treated only ^{28}SiO. The present work discusses preliminary results from a new model that incorporates the three most common isotopomers of SiO, coupled by infra-red line overlap, and replaces the LVG approximation with a spherical radiative transfer model, based on accelerated lambda iteration (ALI).

2 The Model

The current model involves the rotational states $J = 0 - 39$ in vibrational energy levels $v = 0 - 4$ in the isotopomers ^{28}SiO, ^{29}SiO and ^{30}SiO, all of which are radiatively coupled by line overlap. Overlap does not directly couple the purely rotational transitions that may exhibit strong maser action. Overlap of SiO transitions with those of H_2O, or other molecules, are not included.

The LVG maser model has been replaced by a maser-free ALI solution, followed by an independent formal solution for the maser transitions, following the saturation model in [6]. The global spherical radiative transfer solution is arguably a better approximation than LVG, but has the disadvantage that the clump structure made possible by random distribution of LVG sites is lost. Solutions therefore result in simulated VLBI images with circular symmetry.

Physical conditions are derived from the CODEX hydrodynamic solutions (model o54) that are based on a model star with the parameters of o Cet, rather than TX Cam [7]. These models include tables of radial shock positions and stellar photospheric radii. There are three sets of models: the extended and compact atmosphere models, each covering approximately one pulsation period, and a more extensive model, covering 4 periods. Unless stated otherwise, results discussed below are drawn from the compact atmosphere (248-series) models that extend in 14 samples from a phase of -0.30 to a phase of 1.00 including optical maxima at phases 0.00 and 1.00.

3 Results

As in previous models, we find that the flux density of the masers, particularly those in the $v = 1$, 43-GHz transition of the most common isotopomer, roughly follows the optical light curve. We show in Fig. 1 the maser light curves for peak flux density (at any frequency) in the ^{28}SiO $v = 1$ 43-GHz transition. There is one curve for each series, noting that the data for the 260-series (extended atmosphere) is incomplete. Perhaps the main problem with the model light curves is that there is far too much contrast between maser maxima and minima. While the ratio of maximum to minimum flux density is typically ~ 2 in observations of TX Cam [1], it can be several orders of magnitude in the models, with the 248-series in particular spending a considerable phase interval (approximately 0.1–0.4) in a very low state that would be undetectable in observations similar to those of TX Cam. However, large arcs of the maser ring of TX Cam are missing at some phases, showing that large contrasts do occur locally in real stars. The asymmetry of the envelope of a

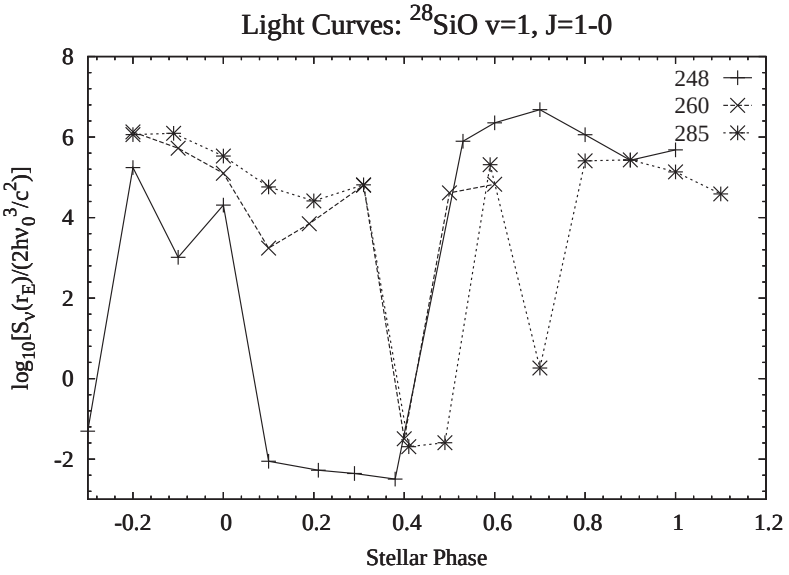

Fig. 1. Peak spectral flux density as a function of stellar phase for the three model cycles considered so far. Series 260 is incomplete. Flux densities are evaluated at a standard distance from the stellar centre of $r_E = 10^{16}$ cm. Symbols mark computed data points

real star likely leads to 'phase mixing', so that it exhibits, at any one phase, features that correspond to a range of phases of an ideal spherical envelope.

Model spectra can be straightforwardly constructed from radial brightness distributions for a particular model series and stellar phase. We have used a plotting format where spectra from all three isotopomers are plotted one above the other in separate panels (see Fig 2). However, spectra for only one vibrational state at a time are shown. The example in Fig. 2 is for $v = 1$, and is the last model of the 248-series, corresponding to a stellar phase of 1.0. The $J = 1 - 0$ spectrum from ^{28}SiO (see bottom panel) should be compared to the observational spectra in [8]. The total spectral extent in the model (40 km s^{-1}) is about twice that in the observations, and the spectrum of TX Cam itself is more strongly double peaked. Qualitative differences between some lineshapes, for example between ^{29}SiO, $J = 2 - 1$ and $J = 1 - 0$ in deserve further investigation.

There are significant differences in detail between the present model and previous versions due to the improved hydrodynamical inputs. A very important example is that the behaviour of the shocks in the present model is not simply a sequence of pulses that move outwards with an almost steady, but slowly reducing radial velocity. One shock, labelled S2 in [7] does behave like this, but another, labelled S1, shrinks from an initial value of 2.03 parent radii to 1.80 over an interval of 0.4 periods. A new shock, S3, appearing at phase 0.6 initially shrinks from 1.13 parent radii to 0.86 over 0.3 periods, before beginning to expand again by the end of the sequence.

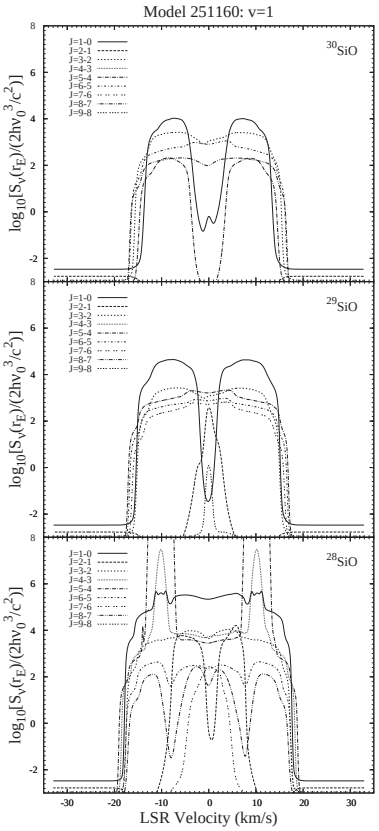

Fig. 2. Spectra from the $v = 1$ vibrational state for the model 251160 of the 248-series, corresponding to an optical stellar phase of 1.0. Flux densities assume a standard distance of $r_E = 10^{16}$ cm from the stellar centre

The behaviour of the 43-GHz maser brightness in $v = 1$ for ^{28}SiO as a function of radius and phase is presented in Fig. 3. During the part of the cycle between phases 0.10 and 0.40, maser emission is faint, and not strongly constrained to any particular radius, though the outer radius of the maser zone has become attached to the outward moving shock, S2, by phase 0.38. At later phases, the shock still defines the outer edge of the maser zone, but has clearly become detached from the ring of brightest emission that has formed by phase 0.53, and then decreases in radius somewhat until phase 1.0. Shocks S1 and S3 remain close to the stellar photosphere and appear to have no influence on the distribution of maser brightness.

Since a ring of brightest emission is sustained for at least half the stellar period at a radius where no shocks are travelling, it is clear that this ring of emission must be pumped primarily by infra-red radiation. However, the outward-moving shock is clearly instrumental in defining the bounds of the maser zone, rendering a considerable shell of material suitable for strong maser action. Material in this

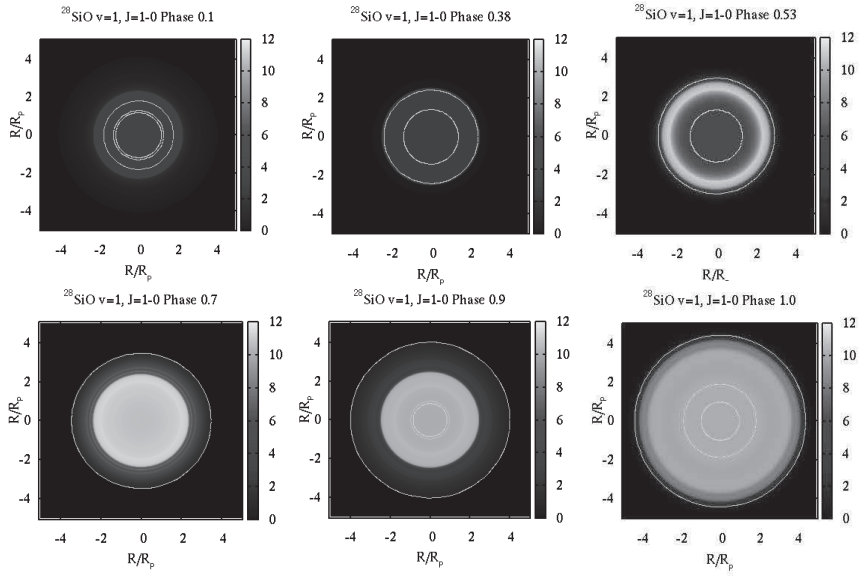

Fig. 3. Radial maser brightness distribution in the 43-GHz $v = 1$ transition of ^{28}SiO at six phases of the model star on the optical scale. White rings mark the positions of shocks and the stellar photosphere. Radii are in units of R_p, the 'parent radius' of a non-pulsating model star. The brightness scale is the $\log_{10}$ of the brightness relative to the transition-dependent group $2h\nu_0^3/c^2$, where ν_0 is the laboratory central frequency of the transition

shell was only weakly inverted in the unshocked gas present during the phase range 0.1–0.4.

A short gif-animation of the maser distribution around the model star, for comparison with the TX Cam movie, is available on request.

The observations in [1] generally show an expansion of the main maser ring in the first half of each pulsation cycle, followed by contraction in the second half. This is consistent with our model if the ring position is defined by shock-driven expansion in the first half-cycle, followed by a contracting, radiation-pumped ring shrinking by a factor of 25 % between phases 0.53 and 1.0. The width of the maser ring also rises in the second half cycle of our model in agreement with observations, though the inner edge of the shell has become very poorly defined by phase 1.0. Bright rings of maser emission are likely associated with atmospheric layers of high mid-infrared opacity.

References

1. *Gonidakis I., Diamond P. J.* A long-term VLBA monitoring campaign of the $v = 1$, $J = 1 - 0$ SiO masers towards TX Cam — I. Morphology and shock waves // MNRAS — 2013. — Vol. 433. — P. 3133–3151.

2. *Humphreys E. M. L., Gray M. D., Yates J. A., Field D., Bowen G., Diamond P. J.* Numerical simulations of stellar SiO maser variability // Astron.& Astrophys. — 2002. — Vol. 386. — P. 256–270.
3. *Bowen G. H.* Dynamical modeling of long-period variable star atmospheres // Astrophys. J. — 1988. — Vol. 329. — P. 299–317.
4. *Gray M. D., Wittkowski M., Scholz M., Humphreys E. M. L., Ohnaka K., Boboltz D.* SiO maser emission in Miras // MNRAS — 2009. — Vol. 394. — P. 51–66.
5. *Ireland M. J., Scholz M., Wood P. R.* On the observability of geometric pulsation of M-type Mira variables // MNRAS — 2004. — Vol. 352. — P. 318–324.
6. *Field D., Gray M. D.* The amplification of celestial maser radiation in the general many-level case // MNRAS — 1988. — Vol. 234. — P. 353–372.
7. *Ireland M. J., Scholz M., Wood P. R.* Dynamical opacity-sampling models of Mira variables — II. Time-dependent atmospheric structure and observable properties of four M-type model series // MNRAS — 2011. — Vol. 418. — P. 114–128.
8. *Gonidakis I., Diamond P. J., Kemball A. J.* Kinematics of the $v = 1$, $J = 1 - 0$ SiO masers at 43 GHz towards TX Cam — a new 73-frame movie // MNRAS — 2010. — Vol. 406. — P. 395–408.